Supplementary Information

A Comparison Between Oestradiol Aptamers as Receptors in CNT FET Biosensors

Erica Cassie,[ab] Hamish Dunham,[c] Erica Happe,[ab] Hong Phan T. Nguyen,[ab] Janet L. Pitman[c] and Natalie O. V. Plank[ab]

[a] *School of Chemical and Physics Sciences, Victoria University of Wellington, Wellington, New Zealand*
[b] *The MacDiarmid Institute for Advanced Materials and Nanotechnology, Wellington, New Zealand*
[c] *School of Biological Sciences, Victoria University of Wellington, Wellington, New Zealand*

This document contains the circular dichroism blanks, gate transfer sweeps, real time sensing measurements, and plots of the change in normalised current upon the addition of analyte against the concentration of analyte in the well after the addition.

1 Circular Dichroism Spectroscopy Blanks

Figure 1 shows the blank spectra that were subtracted from the spectra of the aptamers. Each plot shows 0x, 1x, and 5x concentrations of oestradiol, with no aptamer present. (a) shows the spectra of 0.05x PBS, 5% EtOH, while (b) shows the spectra of 1x PBS, 5% EtOH.

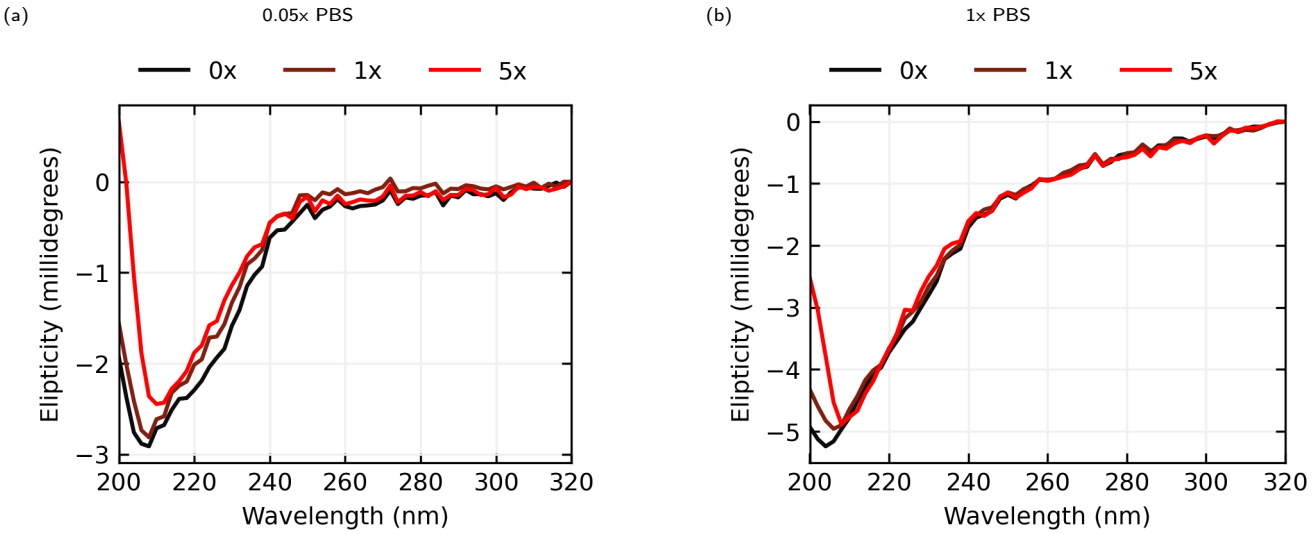

Fig. 1 Circular dichroism spectra for 0x, 1x, and 5x concentrations of E2 with no aptamer in (a) 0.05x PBS and (b) 1x PBS

2 Gate Transfer Sweeps

Each individual sensor presented in the paper is shown. Fig 2 below shows the numbering system to identify each channel on the chip.

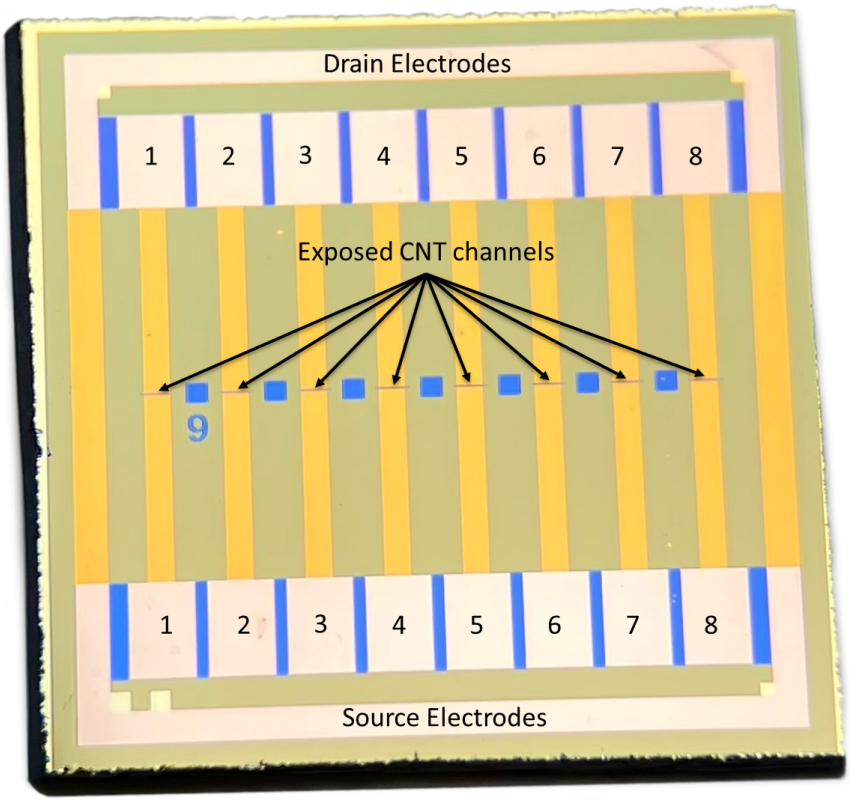

Fig. 2 A chip, like those used in this work, showing the exposed CNT channels and drain and source electrodes of each CNT FET aptasensor. The numbering scheme of devices is annotated over the top of the unencapsulated portion of the electrodes.

Figures 3-5 show gate transfer sweeps taken prior to sensing, plotting I_D against V_{GS}. These are performed in liquid gated conditions, using a Ag/AgCl reference electrode to apply the liquid gate voltage. In all cases $V_{DS} = 100mV$, and V_{GS} is swept from $-0.5V$ to $1V$ and back to $-0.5V$. When the current is negative it is plotted on the same axes in blue. The accuracy limit of the NI PXIe-4138 source measure unit used to make these measurements is is 0.03% + 200 pA, so readings below 200 pA are sometimes negative without this indicating any leakage current in the system. In the case of figure 3 (a) and (b), the gate sweeps shown were taken after sensing. These devices had poor electrical connections during the initial gate sweep, so they were remeasured after sensing. Figures 3-4 show gate transfer sweeps for AL-35 aptasensors. Figure 5 shows gate transfer sweeps for JR-31 aptasensors.

2.1 AL-35 Aptasensors

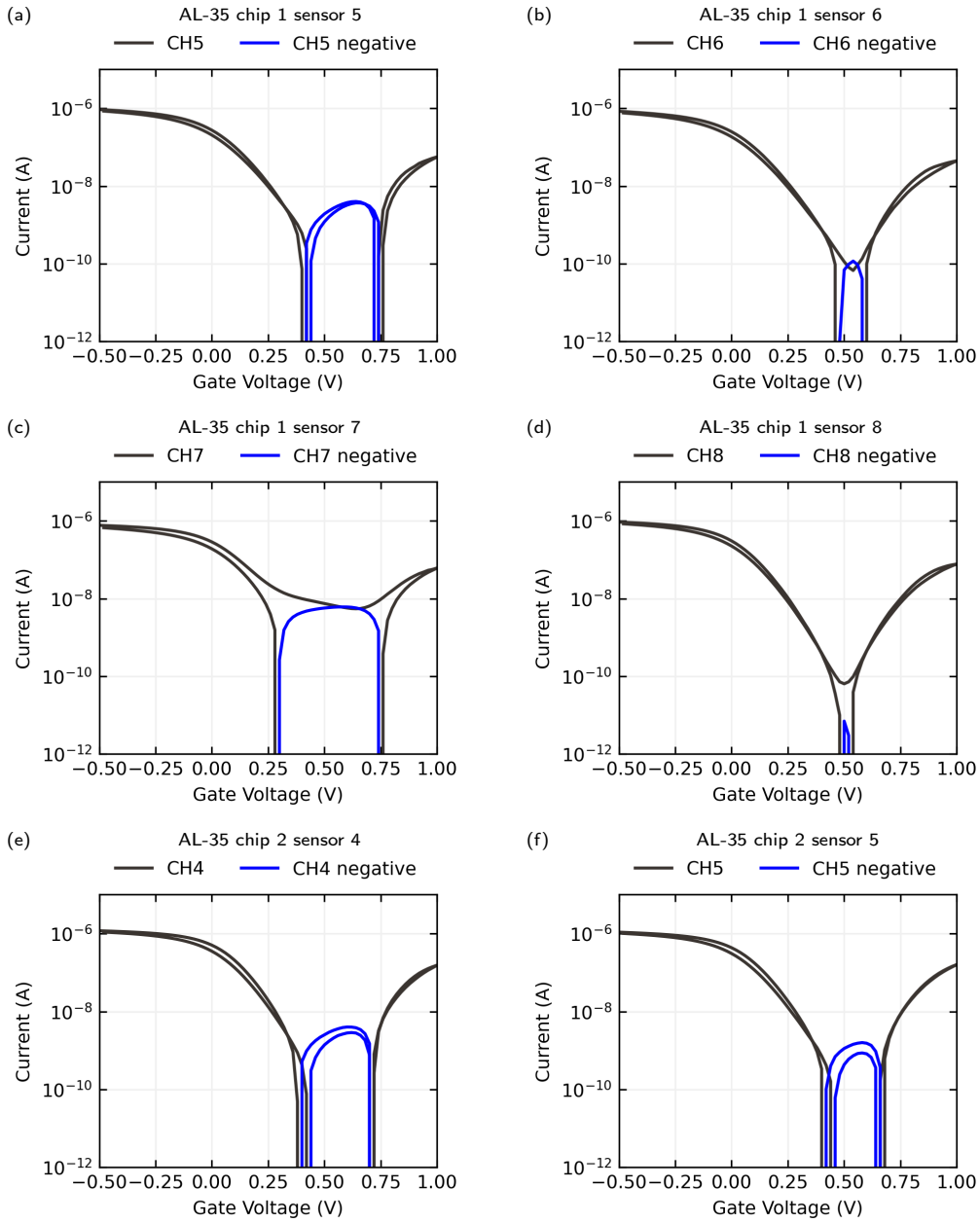

Fig. 3 Gate transfer sweeps for Al-35 aptasensors. (a) and (b) were taken after sensing, (c)-(f) were taken before sensing. (a)-(d) are different sensors on the same chip, chip 1. (e) and (f) are from chip 2. The absolute value of negative currents is plotted in blue.

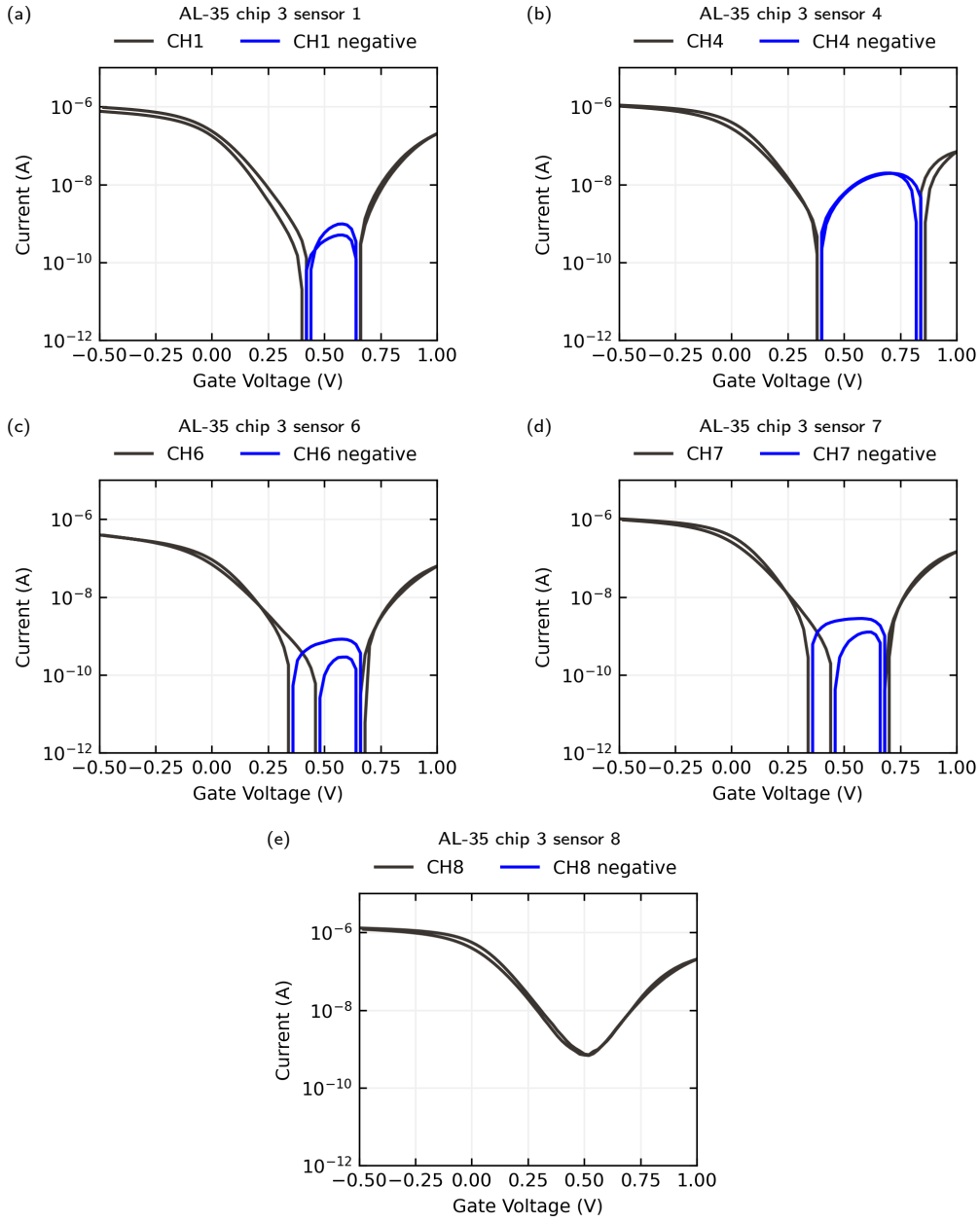

Fig. 4 Gate transfer sweeps for Al-35 aptasensors, taken before sensing. (a)-(e) are from chip 3. The absolute value of negative currents is plotted in blue.

2.2 JR-31 Aptasensors

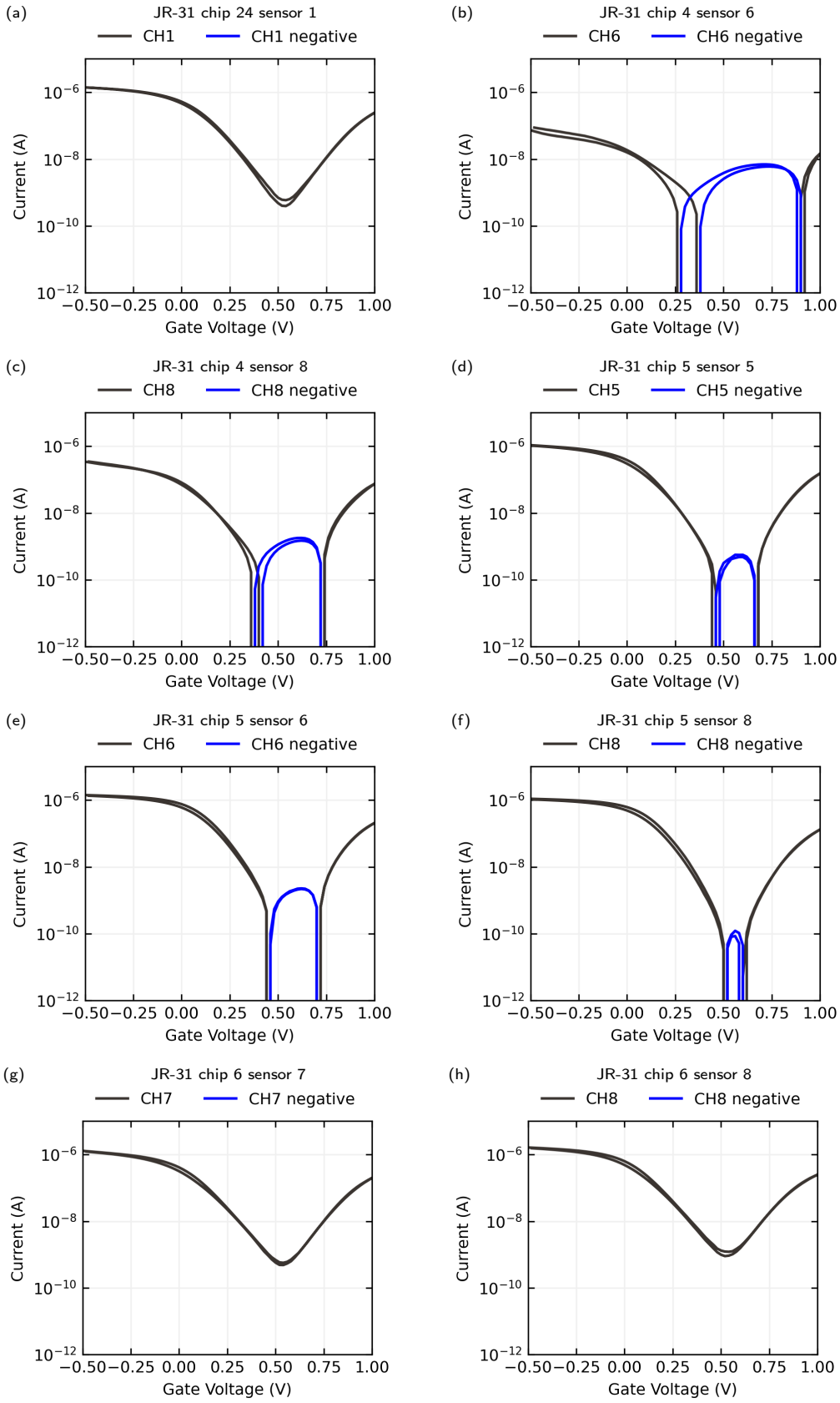

Fig. 5 Gate transfer sweeps for JR-31 aptasensors, taken before sensing. (a)-(c) are different sensors on the same chip, chip 4. (d)-(f) are from chip 5, (g) and (h) are from chip 6. The absolute value of negative currents is plotted in blue.

3 Sensing - Current Against Time Series

Figures 6-8 show normalised current against time data for each sensor with annotations indicating the time of analyte additions and the analyte concentration in the well after the addition. These plots have had outlier points removed. The outlier filter takes a 40 second window about each data point and calculates the median and interquartile range of current within this window, and excludes the data point if it is more than 2.22 times the interquartle range away from the median, equivalent to 3 standard deviations if the distribution of points is Gaussian. This removes spikes in the current caused by external interference in the lab environment, such as the opening and closing of magnetically locked doors. Figures 6-7 show current time series for AL-35 aptasensors. Figure 8 shows current time series for JR-31 aptasensors.

3.1 AL-35 Aptasensors

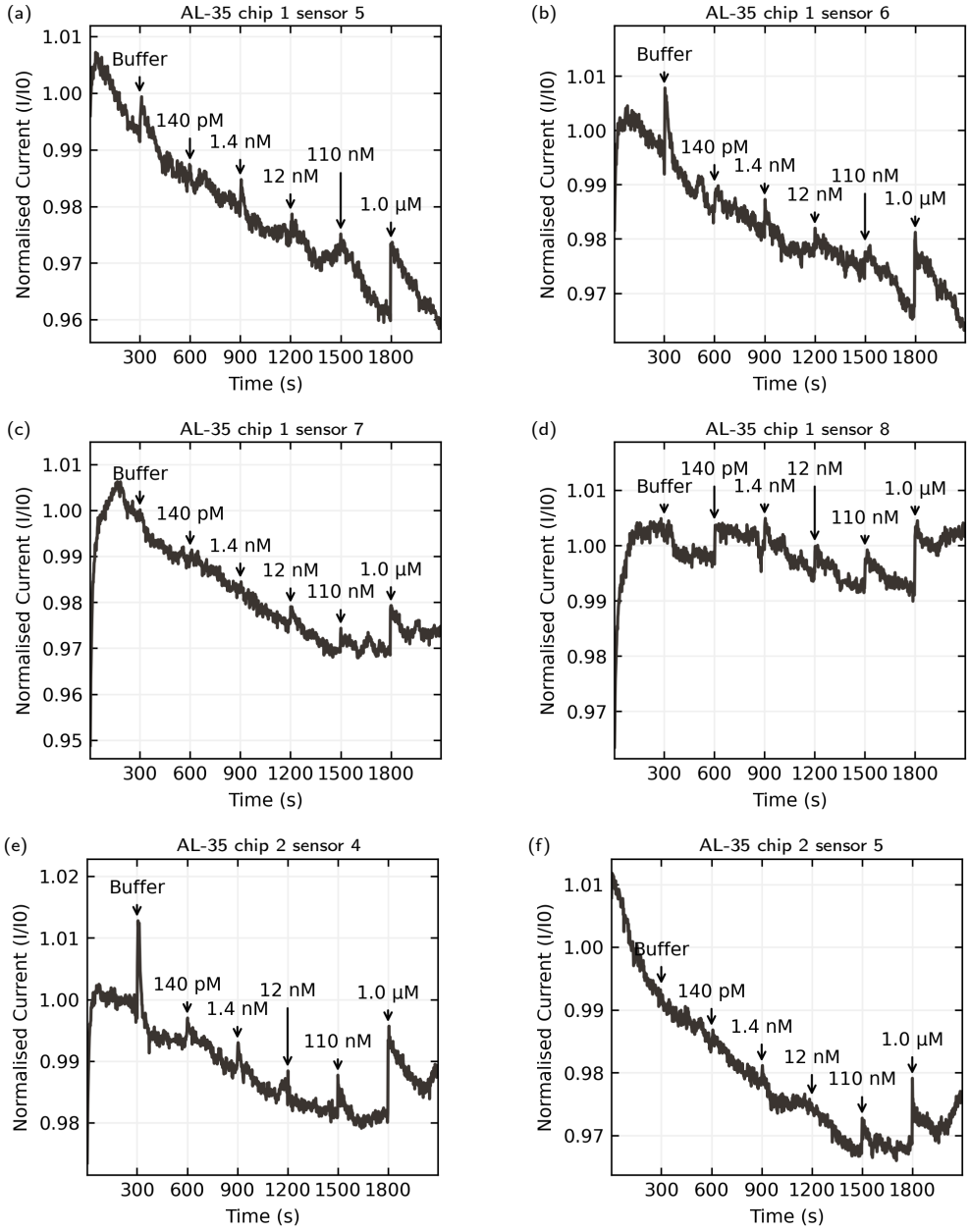

Fig. 6 Sensing results as current time series for Al-35 aptasensors. (a)-(d) are different sensors on the same chip, chip 1. (e) and (f) are from chip 2.

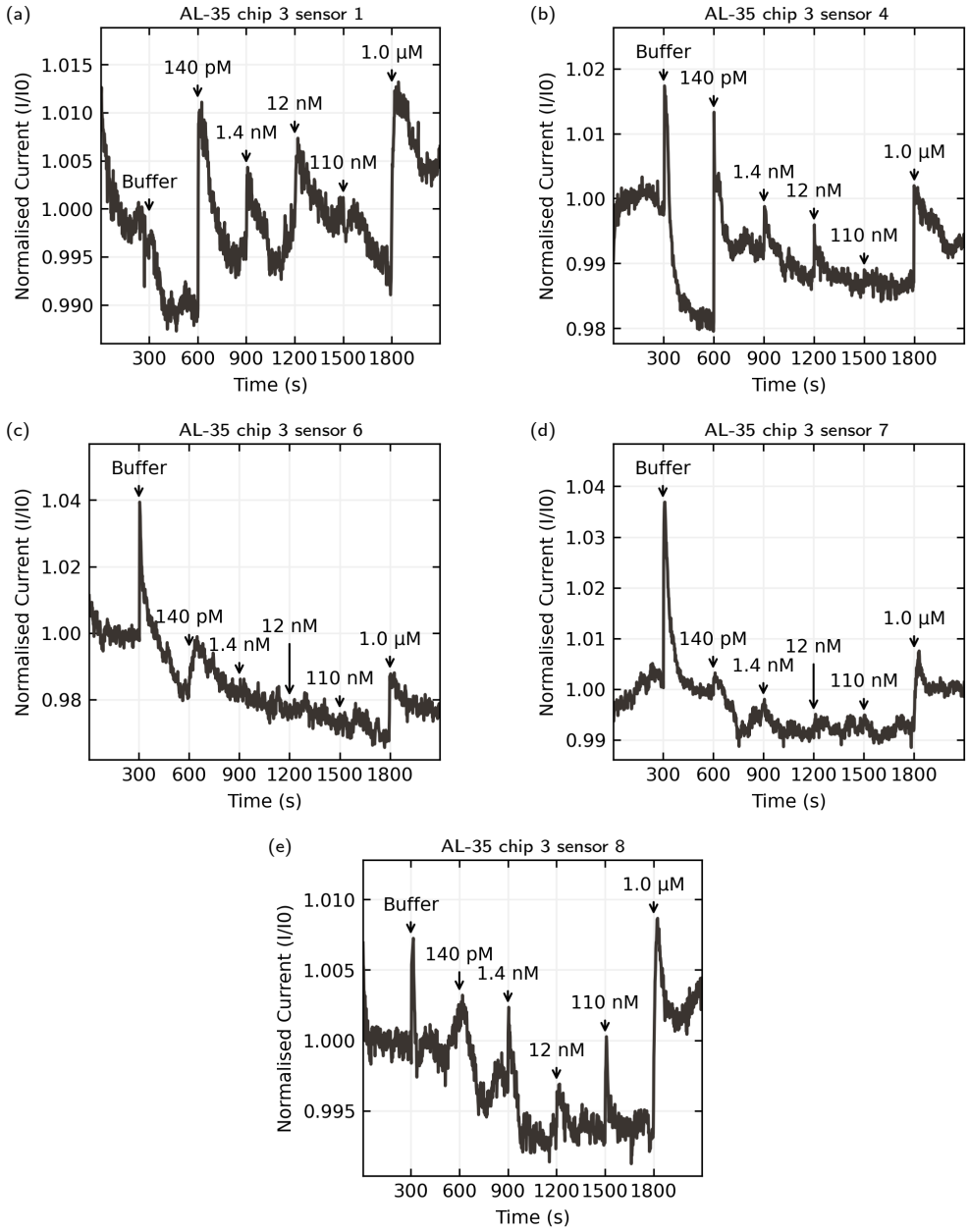

Fig. 7 Sensing results as current time series for Al-35 aptasensors. (a)-(e) are from chip 3.

3.2 JR-31 Aptasensors

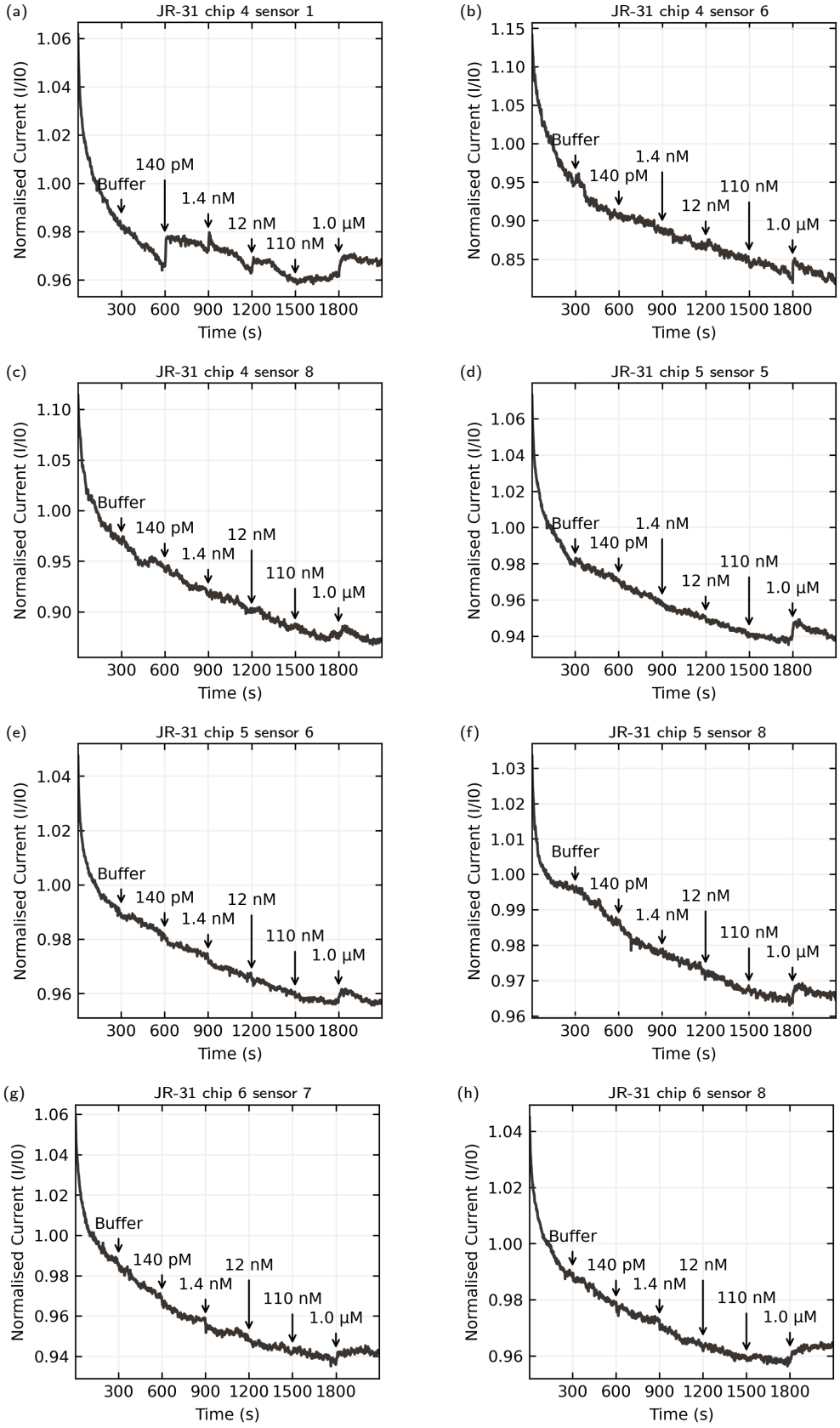

Fig. 8 Sensing results as current time series for JR-31 aptasensors. (a)-(c) are different sensors on the same chip, chip 4. (d)-(f) are from chip 5, (g) and (h) are from chip 6.

4 Sensing - $\Delta I/I_0$ Against E2 Concentration

Figures 9-11 show the step in normalised current upon analyte addition against the concentration of analyte in the well after the addition. These plots are similar to the plots in the main body of the text, however they are calculated in a different way. To calculate these values we start with the current time series. For each analyte addition two windows each with a width of 120 s are used, one finishing 15 s before the addition and one starting 15 s after the addition. The mean of the normalised current within each window is calculated, with the standard deviation taken as the uncertainty, then the value for the window before the addition is subtracted from the value for the window after the addition. The aggregated values shown in the main body of the text group together all sensors based on their receptor, either Al-35 or JR-31, and calculates the mean and standard deviation of their response to each analyte addition. Figures 9-10 show $\Delta I/I_0$ against concentration for AL-35 aptasensors. Figure 11 shows $\Delta I/I_0$ against concentration for JR-31 aptasensors.

4.1 AL-35 Aptasensors

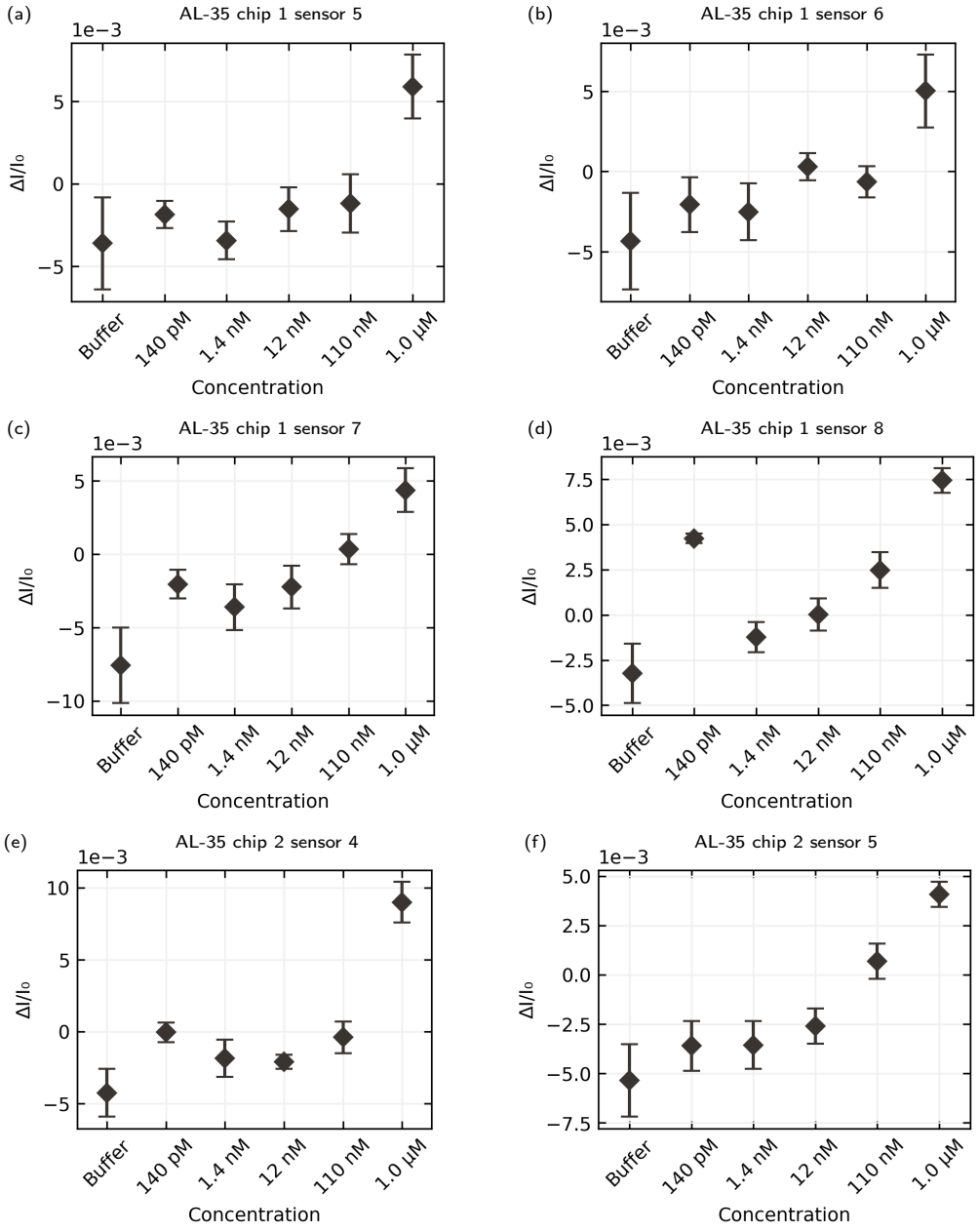

Fig. 9 Sensing results as $\Delta I/I_0$ against E2 concentration for Al-35 aptasensors. (a)-(d) are different sensors on the same chip, chip 1. (e) and (f) are from chip 2.

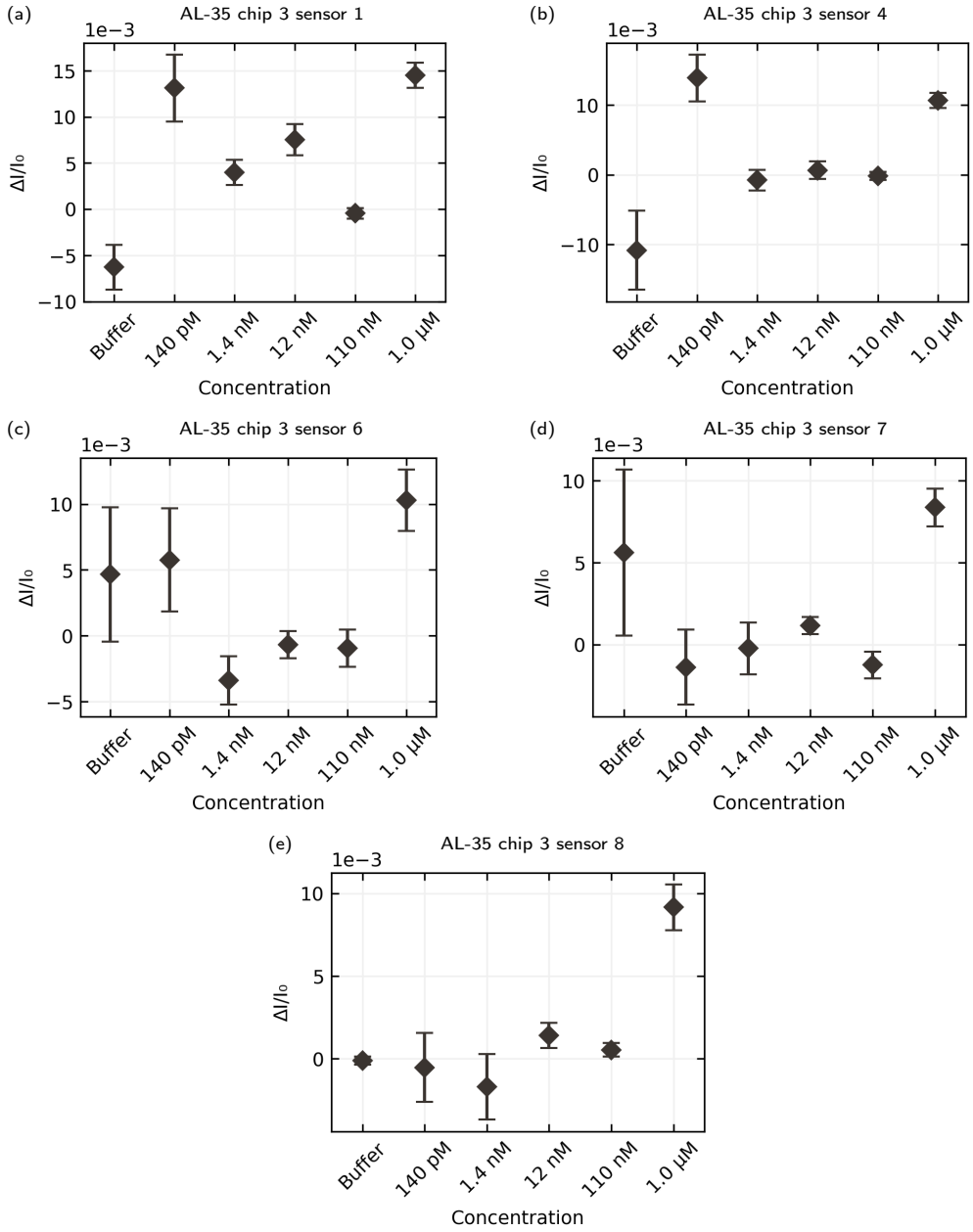

Fig. 10 Sensing results as $\Delta I/I_0$ against E2 concentration for Al-35 aptasensors. (a)-(e) are from chip 3.

4.2 JR-31 Aptasensors

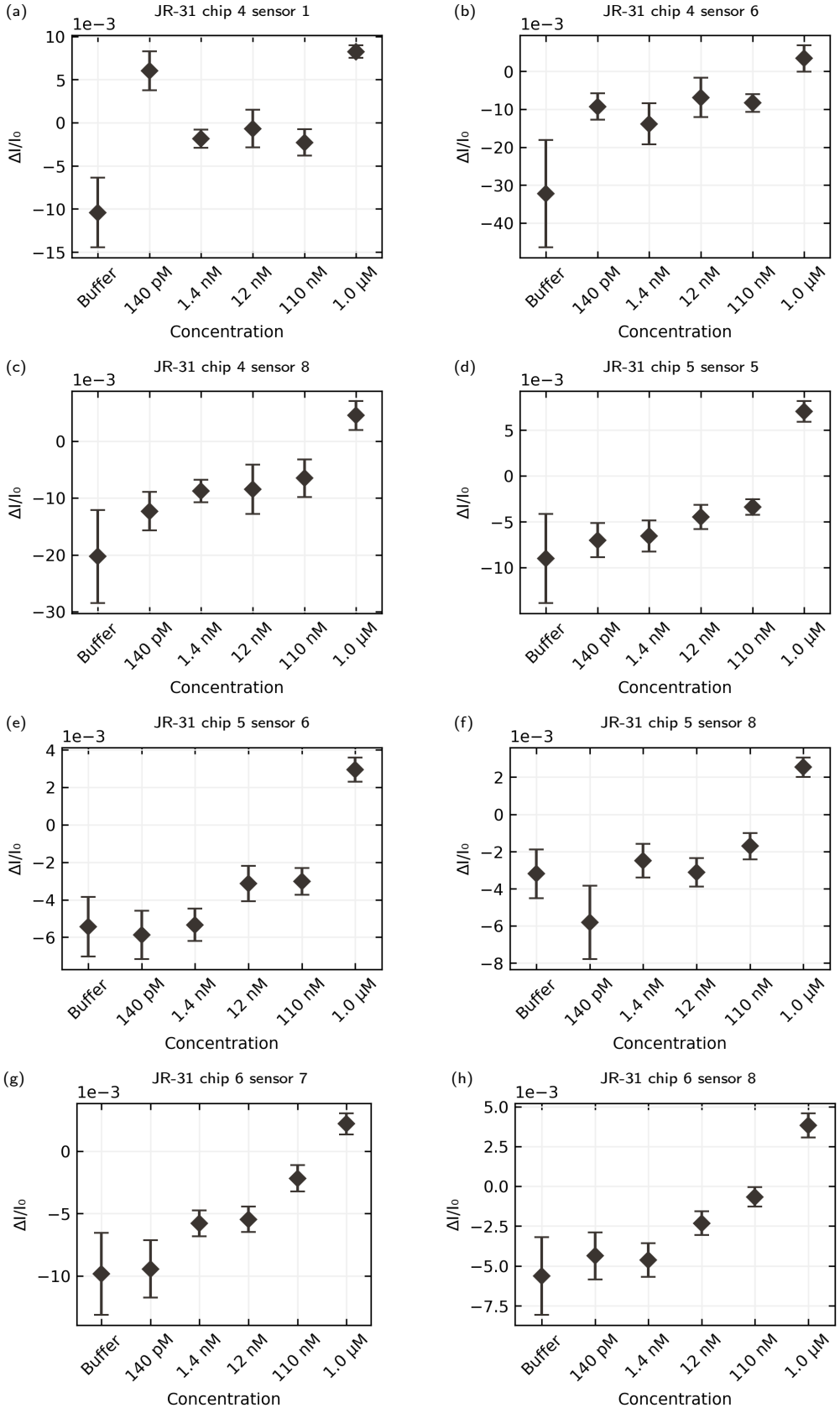

Fig. 11 Sensing results as $\Delta I/I_0$ against E2 concentration for JR-31 aptasensors. (a)-(c) are different sensors on the same chip, chip 4. (d)-(f) are from chip 5, (g) and (h) are from chip 6.